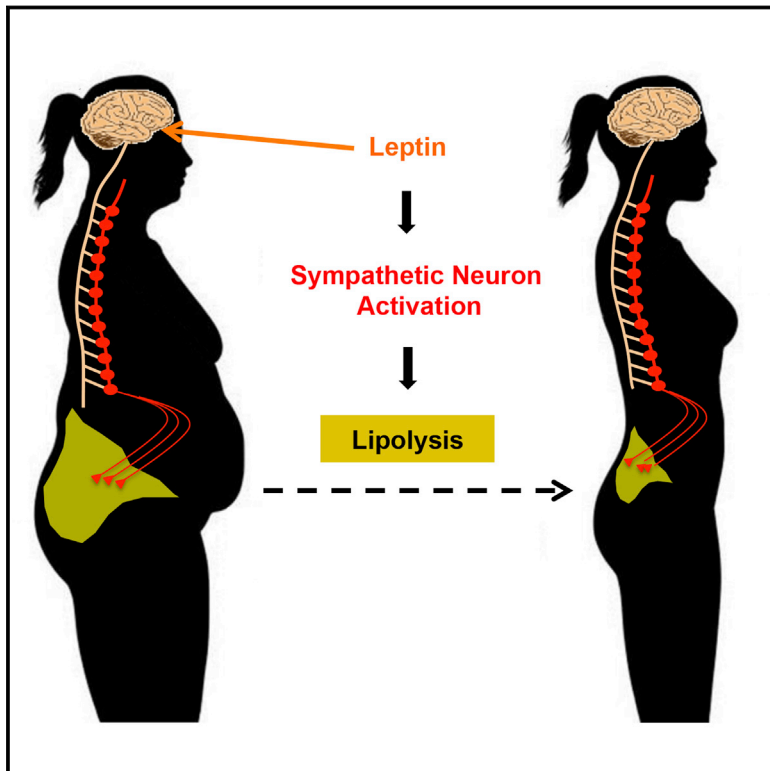


Sympathetic Neuro-adipose Connections Mediate Leptin-Driven Lipolysis

Graphical Abstract



Authors

Wenwen Zeng, Roksana M. Pirzgalska, Mafalda M.A. Pereira, ..., Gabriel G. Martins, Jeffrey M. Friedman, Ana I. Domingos

Correspondence

dominan@igc.gulbenkian.pt

In Brief

The lipolytic effect of leptin is mediated by sympathetic neurons that innervate adipocytes, forming neuro-adipose junctions that directly mediate fat breakdown. Anti-obesity strategies targeting the sympathetic neurons in fat have the potential to circumvent central leptin resistance.

Highlights

- The neuro-adipose junction in white adipose tissue is visualized in vivo
- Adipocyte-projecting neurons can completely envelop an adipocyte
- Leptin stimulates lipolysis via sympathetic neurons in fat
- Optogenetic activation of sympathetic fibers in fat drives lipolysis and fat mass reduction



Sympathetic Neuro-adipose Connections Mediate Leptin-Driven Lipolysis

Wenwen Zeng,^{2,3,7} Roksana M. Pirzgalska,^{1,7} Mafalda M.A. Pereira,¹ Nadiya Kubasova,¹ Andreia Barateiro,^{1,6} Elsa Seixas,¹ Yi-Hsueh Lu,² Albina Kozlova,² Henning Voss,⁵ Gabriel G. Martins,⁴ Jeffrey M. Friedman,^{2,3,8} and Ana I. Domingos^{1,8,*}

¹Obesity Laboratory, Instituto Gulbenkian de Ciência, Oeiras 2780-156, Portugal

²Laboratory of Molecular Genetics, The Rockefeller University, New York, NY 10021, USA

³Howard Hughes Medical Institute, The Rockefeller University, New York, NY 10021, USA

⁴Advanced Microscopy Unit, Instituto Gulbenkian de Ciência, Oeiras 2780-156, Portugal

⁵Department of Radiology, Weill Cornell Medical College, New York, NY 10021, USA

⁶Research Institute for Medicines (iMed.Ulisboa), Faculty of Pharmacy, Universidade de Lisboa, Avenue Professor Gama Pinto, Lisbon 1649-003, Portugal

⁷Co-first author

⁸Co-senior author

*Correspondence: dominan@igc.gulbenkian.pt

<http://dx.doi.org/10.1016/j.cell.2015.08.055>

SUMMARY

Leptin is a hormone produced by the adipose tissue that acts in the brain, stimulating white fat breakdown. We find that the lipolytic effect of leptin is mediated through the action of sympathetic nerve fibers that innervate the adipose tissue. Using intravital two-photon microscopy, we observe that sympathetic nerve fibers establish neuro-adipose junctions, directly “enveloping” adipocytes. Local optogenetic stimulation of sympathetic inputs induces a local lipolytic response and depletion of white adipose mass. Conversely, genetic ablation of sympathetic inputs onto fat pads blocks leptin-stimulated phosphorylation of hormone-sensitive lipase and consequent lipolysis, as do knockouts of dopamine β -hydroxylase, an enzyme required for catecholamine synthesis. Thus, neuro-adipose junctions are necessary and sufficient for the induction of lipolysis in white adipose tissue and are an efferent effector of leptin action. Direct activation of sympathetic inputs to adipose tissues may represent an alternative approach to induce fat loss, circumventing central leptin resistance.

INTRODUCTION

White adipose tissues (WATs) serve as a storage depot for energy-rich triglycerides. In times of privation, this lipid storage can be released as part of an adaptive response to the energy shortage. Lipolysis, the process of hydrolyzing stored triglycerides in adipocytes, is regulated by several G-protein-coupled receptors, including adrenergic receptors, all of which activate protein kinase A (PKA) and elevate the intracellular levels of cyclic adenosine monophosphate (cAMP) (Brasaemle, 2007). PKA also phosphorylates several key target proteins, including

lipid-droplet-associated protein perilipin, hormone-sensitive lipase (HSL), and a set of esterases that collectively promote the hydrolysis of triglycerides into free fatty acids (FFAs) and glycerol, which are then released into plasma to meet the energy demands of other tissues (Brasaemle, 2007). HSL is a canonical target of PKA in adipocytes, and this enzyme catalyzes the conversion of diacylglycerol to monoacyl glycerol (Brasaemle, 2007).

Adipose tissue mass is homeostatically controlled by an endocrine loop in which leptin acts on neural circuits in the hypothalamus and elsewhere in brain to regulate food intake and peripheral metabolism (Friedman and Halaas, 1998). In wild-type (WT) and leptin-deficient *ob* animals, leptin treatment reduces food intake and leads to a rapid depletion of fat mass (Halaas et al., 1995, 1997; Montez et al., 2005). Of note, the depletion of fat mass after leptin treatment is distinct from that observed after food restriction in a number of respects: leptin treatment spares lean body mass and also potentially stimulates glucose metabolism, while starvation results in a loss of lean body mass and causes insulin resistance (Newman and Brodows, 1983; Koffler and Kisch, 1996; Awad et al., 2009; Elia et al., 1999). In addition, leptin-deficient *ob/ob* mice pair-fed to leptin-treated *ob* mice lose only half the weight of those treated with leptin, further implicating a mechanism beyond a reduced food intake (Rafael and Herling, 2000). Because leptin has been shown to increase the sympathetic efferent signal to brown adipose tissues (BAT) (Scarpace and Matheny, 1998; Rezaei-Zadeh and Münzberg, 2013), it has been suggested that leptin also activates sympathetic efferents to WAT to increase lipolysis in WAT. However, this has not been directly shown, and the nature of the effector mechanism underlying leptin-stimulated lipolysis in WAT has not been defined. In particular, it has not been established whether the increased lipolysis in WAT in response to leptin is due to a circulating hormone (or hormones) such as norepinephrine (NE) and/or another mediator that is released either centrally or peripherally (adrenal gland or macrophages), or specific efferent neural inputs to WAT, which mediates central leptin action. However, the effect of leptin on energy balance does not

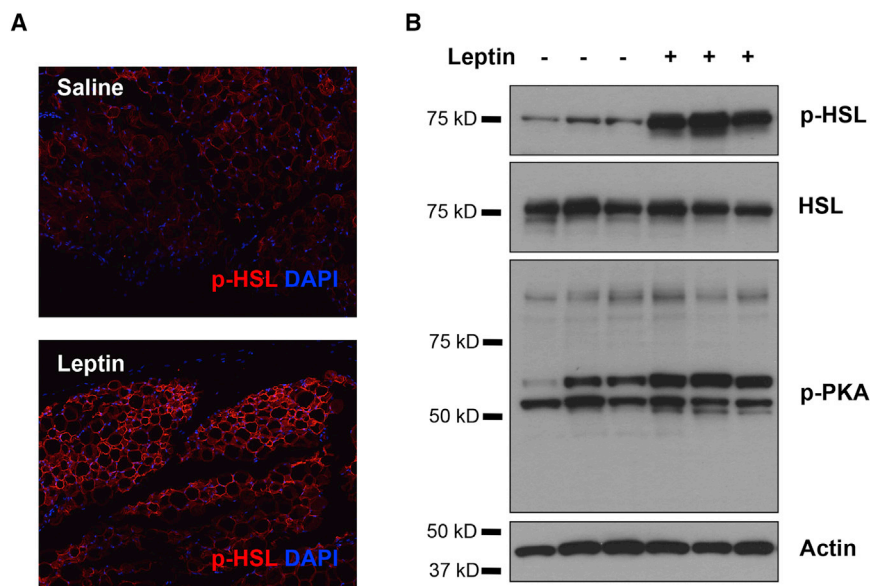


Figure 1. Leptin Stimulates HSL Phosphorylation in WAT

(A) Immunostaining of p-HSL (red) in paraffin sections of epididymal fat of C57Bl6/J mice that were peripherally administrated with 500 ng/hr recombinant leptin for 2 days. (B) p-HSL and phosphorylated PKA substrates in total protein extracts of epididymal fats were examined by immunoblot analysis.

tion of sympathetic inputs to adipose tissues as a strategy for the induction of fat loss.

RESULTS

Phosphorylation of HSL in WAT as a Lipolysis Marker for Leptin Action

To directly assess the cellular effect of leptin on lipolysis in white adipocytes and provide a marker for leptin action, we

require the presence of intact adrenals, suggesting that this organ is unlikely to be the source of the lipolytic signal (Arvaniti et al., 1998).

While numerous previous studies have shown dense neural innervation of BAT, both functionally and anatomically, the innervation of WAT has been difficult to visualize. Thus, it has been suggested that neural inputs to WAT are either very sparse or difficult to be distinguished from en passant axons with terminals on other cell types, such as those in vasculature (Bartness et al., 2005; Bartness and Song, 2007; Youngstrom and Bartness, 1995; Giordano et al., 1996). Indeed, some reports have suggested that the only innervation of WAT is perivascular and that white adipocytes themselves are not directly innervated (Giordano et al., 2005). This controversy has heightened the uncertainty as to the relative roles of sympathetic neural activity to regulate WAT metabolism. Alternatively, macrophages in adipose tissue account for about 10% of the stromal vascular fraction (SVF); hence, local catecholamines produced by these cells could also contribute to lipolysis in WAT in vivo (Weisberg et al., 2003; Nguyen et al., 2011). Thus, the dramatic decrease of adipose tissue mass observed after leptin treatment could, in principle, be mediated by catecholamines or other mediators that are either locally produced or produced by neurons.

In this study, we use anatomic, optogenetic, biochemical, and genetic approaches to show that the catecholamines released at heretofore-unidentified neuro-adipose junctions mediates the lipolytic effect of leptin, thus establishing the effector mechanism underlying the depletion of fat mass by leptin and, potentially, other stimuli. Our data demonstrate that the local sympathetic activity in WAT is necessary and sufficient for the lipolytic effect of leptin. In addition, genetic evidence shows that the β -adrenergic, but not α -adrenergic, receptors partially constitute a signaling pathway that accounts for the lipolytic effect of leptin. Moreover, the effect of pre-synaptic manipulations, such as neural gain of function or loss of function, is more profound than that of post-synaptic manipulations, thus suggesting direct activa-

tion of sympathetic inputs to adipose tissues as a strategy for the induction of fat loss. We searched for biochemical responses in white adipocytes that were specifically activated by leptin treatment. We used a battery of phospho-specific antibodies and found that the phosphorylation of HSL was robustly increased in adipose tissue in response to leptin treatment. Note that our ability to define a biochemical effect of leptin is dependent on the quality of the antibodies, and we found that the anti-pHSL antibody was extremely robust. As shown, peripheral administration of leptin led to a significant increase of phosphorylated HSL (p-HSL) in WAT that could be visualized by immunohistochemistry (Figure 1A) and quantified by immunoblot analysis (Figure 1B). We set out to investigate whether the effect of leptin to increase HSL phosphorylation was mediated by neural efferent outputs onto WAT.

Axonal Bundles Project to WAT and Form Sympathetic Neuro-adipose Junctions

We first used tomography methods to determine whether fat pads were innervated. By coupling optical projection tomography (OPT) to a fat-clearing method that renders whole organs transparent, we were able to macroscopically visualize and document the nerve bundles that innervate the inguinal fat pad (Figure 2A; Experimental Procedures; Supplemental Experimental Procedures for details) (Gualda et al., 2013; Quintana and Sharpe, 2011). A full series of projections of the whole organ are acquired from multiple angles, typically 800–1,600 angles, and from this series of projections, a stack of axial slices can be visualized through back-projection reconstruction (Figure 2B).

From an OPT series of coronal optical sections of inguinal fat organ, we performed a 3D reconstruction, which enabled the visualization of thick axon bundles targeting the fat pad (Figures 2C and 2D). Axon bundles can be identified based on the gray threshold level and morphological features that distinguish them from the vasculature (Figure 2E). These structures within the fat were then segmented using semi-automated software (see Experimental Procedures).

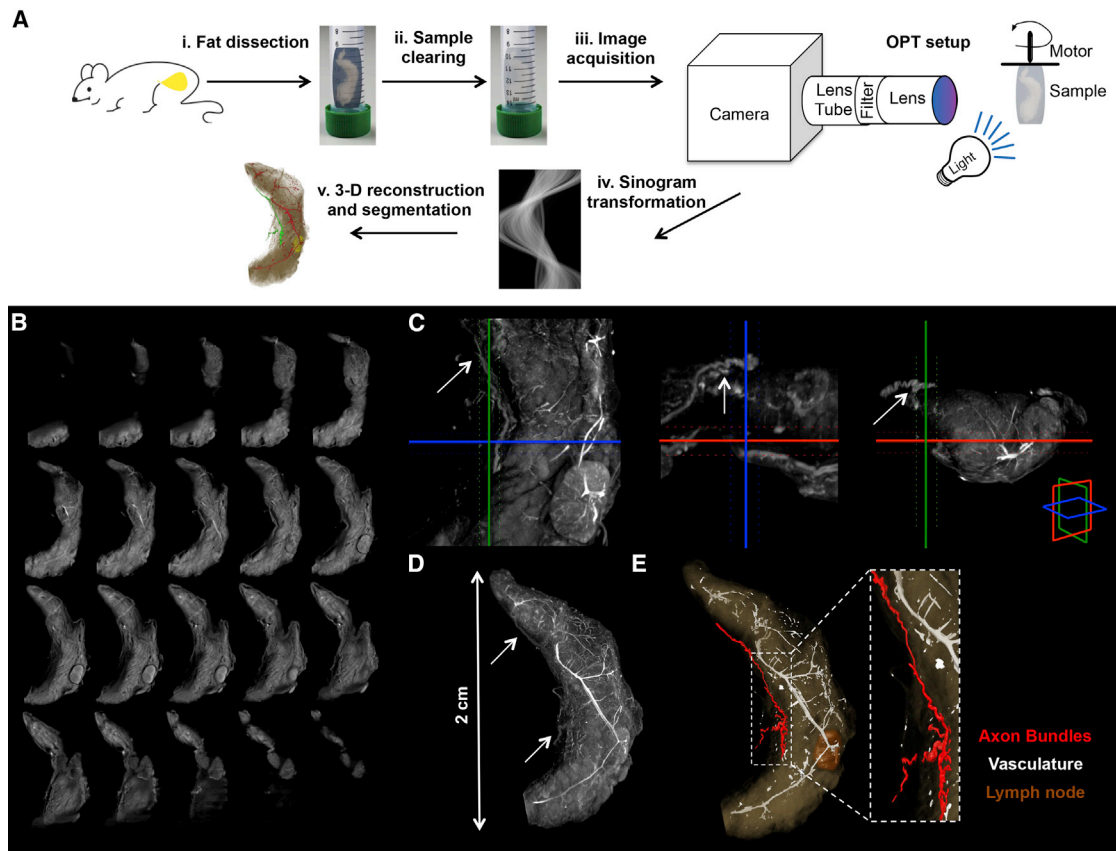


Figure 2. Neural Projections in Fat Detected with OPT

(A) Schematic representation of the OPT method applied to the subcutaneous inguinal fat. (i) Tissue dissection. (ii) Sample clearing. (iii) Image acquisition. (iv) Sinogram transformation. (v) 3D reconstruction and segmentation.

(B) OPT series of coronal sections of inguinal fat organ after 3D reconstruction.

(C) Orthogonal 400- μ m OPT slabs of inguinal fat in coronal, axial, and sagittal views. Axon bundles were identified based on the gray threshold level (arrows).

(D) 3D reconstruction in maximal intensity projection of the OPT coronal sections.

(E) Surface view of segmented structures within inguinal fat.

The neural bundles were micro-dissected from the subcutaneous fat pads and subjected to immunostaining for tyrosine hydroxylase (TH), a marker of sympathetic neurons, and β 3-tubulin (Tub-3), a general marker for the peripheral nervous system (PNS) (Figure 3A). We found that, overall, \sim 50% of the Tub-3-positive neurons also expressed TH, thus establishing the presence of both catecholaminergic and non-catecholaminergic axons innervating subcutaneous fat pads (Figure 3A). Then, we used multiphoton microscopy on the intact inguinal WAT of a living mouse to visualize sympathetic neuro-adipose connections (Figures 3B and 3C; Experimental Procedures). We labeled adipocytes with LipidTOX, a lipophilic dye, and sympathetic axons by crossing TH Cre-recombinase mice (*TH-Cre*) with a Tdtomato-reporter line (*Rosa26-LSL-Tdtomato*) (Figure 3C). We observed that Tdtomato-positive axons in fat pads made dense contacts with adipocytes through bouton-like structures that had the anatomic appearance of neuro-adipocyte junctions, resembling synapses (Figure 3C). We quantified these from eight independent two-photon micrographs and determined that $8\% \pm 4.6\%$ of adipocytes are in direct contact with sympathetic nerves.

Optogenetic Stimulation of Sympathetic Inputs to WAT Leads to Catecholamine Release, HSL Phosphorylation, and Fat Mass Depletion

We assessed the function of the catecholaminergic fibers by crossing the *TH-Cre* mice to a channelrhodopsin (ChR2) reporter line, *Rosa26-LSL-ChR2-YFP*. ChR2-YFP (yellow fluorescent protein) showed a complete co-localization with the endogenous TH, as determined by immunostaining of YFP and TH (Figure 4A). ChR2-YFP-expressing axons that projected onto subcutaneous WAT were then optogenetically activated using a subcutaneously implanted optical fiber targeting the right inguinal fat depot (see Experimental Procedures for surgical details).

While optogenetic tools have been widely used in the CNS, it has not been used as frequently to probe the function of peripheral cells, including sympathetic neurons. We began by validating the use of optogenetic stimulation of sympathetic neurons in primary cultures of superior cervical ganglia (SCG) of *TH-Cre* X *Rosa26-LSL-ChR2-YFP* mice; SCG can be dissected with less difficulty compared to other sympathetic ganglia (see Supplemental Experimental Procedures for culture details). We found

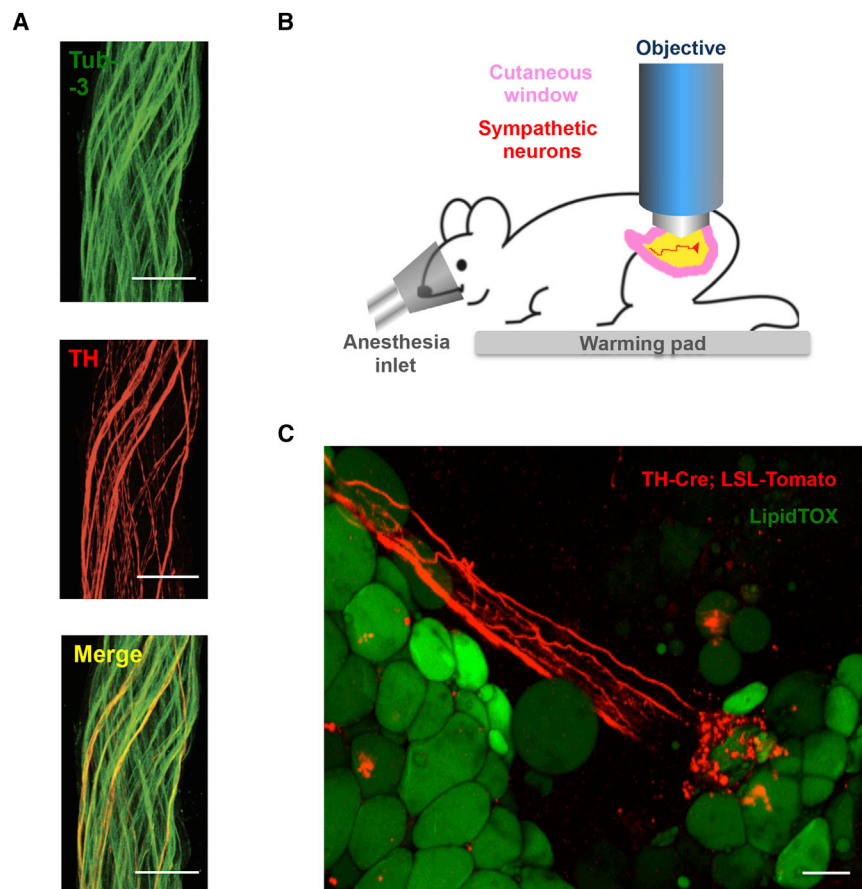


Figure 3. Catecholaminergic Neurons Innervating Adipocytes Integrate Nerve Bundles of Mixed Molecular Identity

(A) Partial co-localization of TH (red), an SNS marker, and Tub-3 (green), a general PNS marker, shown by immunohistochemistry of nerve bundles dissected from the inguinal fat pads of WT mice. Scale bars, 50 μ m.

(B) Schematic representation of the two-photon intra-vital imaging of neurons in the inguinal fat pad.

(C) Intra-vital two-photon microscopy visualization of a neuro-adipose connection in the inguinal fat pad of a live *TH-Cre; LSLs-Tomato* mouse; LipidTOX (green) labels adipocytes. Scale bar, 100 μ m.

that optogenetic stimulation of cultured sympathetic neurons increased expression of c-Fos, a marker for neuronal activity, in TH-positive cells and significantly stimulated NE release *ex vivo*, as assayed with ELISA (Figures 4B and 4C). NE release of ChR2-positive neurons was significantly higher relative to that of ChR2-negative cells (749.6 ± 170.1 pg/ml versus 4.8 ± 1.7 pg/ml, $p < 0.05$) (Figures 4B and 4C; see [Experimental Procedures](#) for culture and stimulation details).

Next, we stimulated ChR2-YFP-expressing axons *in vivo* unilaterally by placing optical fibers subcutaneously, aiming at inguinal fat pads located in the supra-pelvic flank of *TH-Cre X Rosa26-LSL-ChR2-YFP* mice (see [Experimental Procedures](#) for stimulation details). Activation of the ChR2-positive axons in subcutaneous WAT led to a significant increase of NE in the stimulated fat pad, relative to the contralateral un-stimulated control side (2.7 ± 0.5 versus 1.1 ± 0.2 , $p < 0.05$; Figure 4D). We also observed a significant increase of HSL phosphorylation of fat on the side ipsilateral to the optical fiber, compared to the contralateral un-stimulated side (Figure 4E). These data show that local activation of catecholaminergic inputs to fat could locally mimic the biochemical effect of leptin (Figures 4D and 4E). Then, we tested whether a more prolonged (4-week) optogenetic stimulation of ChR2-positive neurons in WAT could deplete fat mass (Figure 4F). The optical stimulation protocol was set to deliver light for every other second at 20 Hz, and

the volume of subcutaneous WAT was determined using MRI with 3D reconstruction (Figures 4F and 4G; see [Experimental Procedures](#) for details). After chronic activation, the size of the optogenetically stimulated ipsilateral fat pads of *TH-Cre; Rosa26-LSL-ChR2-YFP* mice was $23\% \pm 3.4\%$ that of the contralateral control side, representing a statistically and biologically significant decrease in fat mass (Figures 4F and 4G, $p < 0.0001$). This effect depended on ChR2 expression, as the fat pad volume of stimulated fat pads in ChR2-negative mice was unchanged ($86\% \pm 4.3\%$ of the size of the contralateral control fat pad), ruling out a potential nonspecific effect of laser stimulation (Figure 4G; see [Experimental Procedures](#) for details). Together, the results provide anatomical and functional evidence that there are synapse-like sympathetic inputs onto white adipocytes and that their activation is sufficient to promote local NE release, HSL phosphorylation, and a reduction in the mass of an adipose tissue depot.

Local Sympathetic Inputs Are Required for Leptin-Stimulated HSL Lipolysis in WAT

Similarly to optogenetic stimulation of sympathetic innervation in white fat, leptin treatment led to an increase in NE levels in the subcutaneous adipose organ. NE levels in WATs dissected from leptin-treated animals were significantly higher than those in controls (78.7 ± 16.8 pg NE/ μ g of protein versus 30.7 ± 4.1 pg NE/ μ g of protein, $p < 0.05$; Figure 5A). Interestingly, leptin treatment did not affect serum NE levels (Figure 5B), indicating that leptin locally increases NE release in white fat, but not systemically.

Next, we evaluated whether sympathetic activation is necessary for leptin-stimulated lipolysis by disrupting the neural inputs in WAT, using a pharmacologic blockade or local genetic ablation. First, we observed that administration of hexamethonium, a non-depolarizing anti-cholinergic ganglion blocker, significantly decreased the leptin-stimulated phosphorylation of HSL

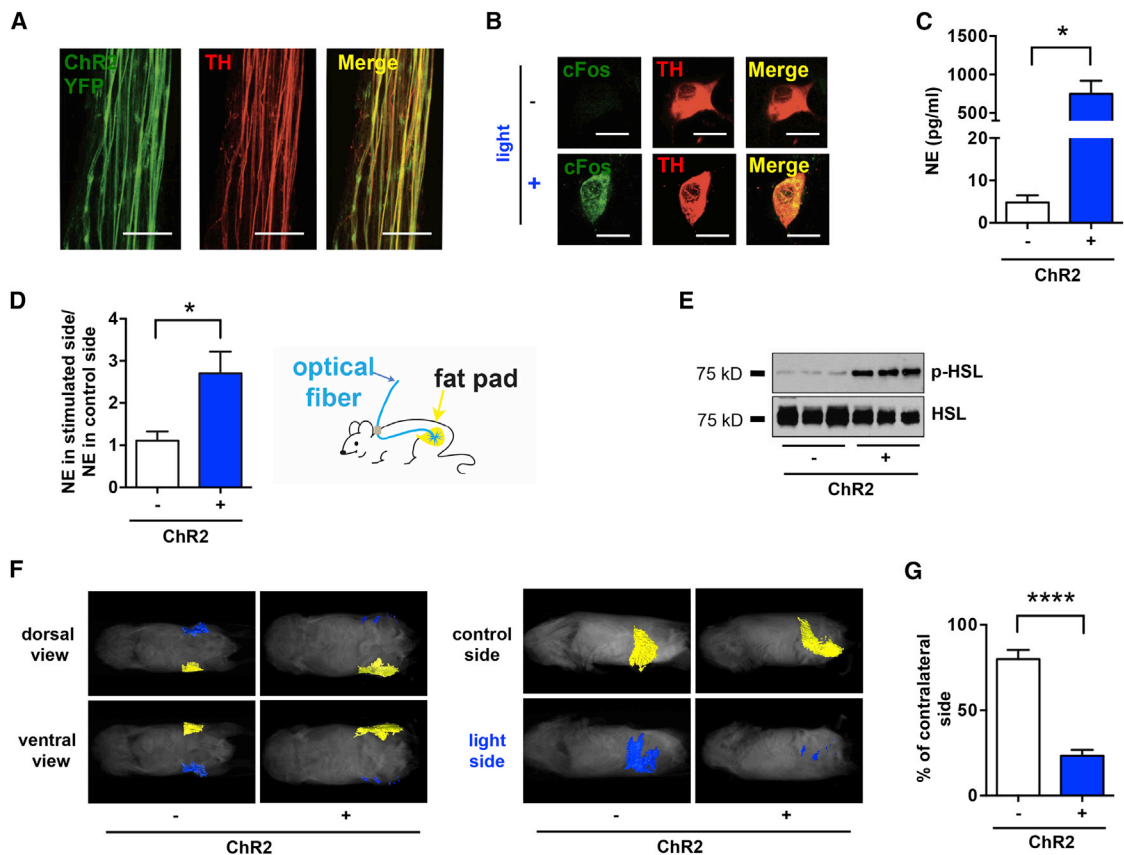


Figure 4. Optogenetic Stimulation of SNS Neurons in Fat Is Sufficient to Drive Lipolysis

(A) Complete co-localization of YFP (green) and TH (red) shown by immunohistochemistry of nerve bundles dissected from the inguinal fat pads of *TH-Cre; LSL-ChR2-YFP*. Scale bars, 50 μ m.

(B) c-Fos (green) induction in cultured SNS neurons after optogenetic activation. Scale bars, 10 μ m.

(C) Ex vivo NE release upon optogenetic stimulation of sympathetic SCG explants isolated from *TH-Cre; LSL-ChR2-YFP* mice and *LSL-ChR2-YFP* control mice ($^*p < 0.05$; $n = 3-6$). Results are shown as mean \pm SEM.

(D) In vivo NE release in subcutaneous fat upon optogenetic stimulation of sympathetic neurons in WATs of *TH-Cre; LSL-ChR2-YFP* and *LSL-ChR2-YFP* control mice that were subcutaneously implanted with optical fibers targeting the inguinal fat pad ($^*p < 0.05$; $n = 8$). Results are shown as mean \pm SEM.

(E) Immunoblot analysis of p-HSL in total protein extracts of subcutaneous fats of *TH-Cre; LSL-ChR2-YFP* and *LSL-ChR2-YFP* control mice that were subcutaneously implanted with optical fibers targeting the inguinal fat pad and optogenetically stimulated for 2 weeks (details are given in [Experimental Procedures](#)).

(F) MRI-guided visualization of fat in *TH-Cre; LSL-ChR2-YFP* and *LSL-ChR2-YFP* control mice that were optogenetically stimulated for 4 weeks (yellow indicates control inguinal fat pad, blue indicates light-stimulated fat pad; details are given in [Experimental Procedures](#)).

(G) Quantification of fat reduction in stimulated side versus the contralateral control side ($^{****}p < 0.0001$; $n = 6$). Results are shown as mean \pm SEM.

See also [Movies S1](#) and [S2](#).

in adipose tissue ([Figure 5C](#)). However, as the action of hexamethonium is systemic and is not cell type specific, affecting all ganglionic transmission, we took a complementary approach by introducing a local neural crush injury to the fibers innervating epididymal fat pads. Because of the anatomy of the fat pad, nerve fibers in the distal portion of the tissues can be efficiently eliminated by a surgical crush of the perivascular axons running parallel to the main vessels (see [Experimental Procedures](#)). We carried out physical denervation with a forcep crushing the fibers 2 mm from the distal tip for 30 s. Leptin was delivered 3 days post-surgery through osmotic pump for 2 days. Consistent with the effect of hexamethonium, after a crush injury to the local nerve, leptin treatment failed to increase HSL phosphorylation on the denervated side compared to the intact contralateral control

([Figure 5D](#)). This showed that local neural activation to WAT is required for the biochemical changes associated with leptin treatment.

To confirm that leptin-mediated lipolysis is the result of activation of sympathetic neural outputs to fat, we ablated these neurons by crossing the *TH-Cre* line with the diphtheria toxin receptor (*DTR*) mice, *Rosa26-LSL-DTR*, and injected diphtheria toxin (DT) locally in subcutaneous inguinal WAT ([Buch et al., 2005](#)). Local treatment with DT eliminated only those sympathetic axons in the regions of the injection site, without effects on other local neuronal populations as shown by the sparing TH-negative Tub-3-positive axons at the site of injection ([Figure 5E](#), $p < 0.001$; see [Supplemental Experimental Procedures](#) for details). These injections were administered peripherally at

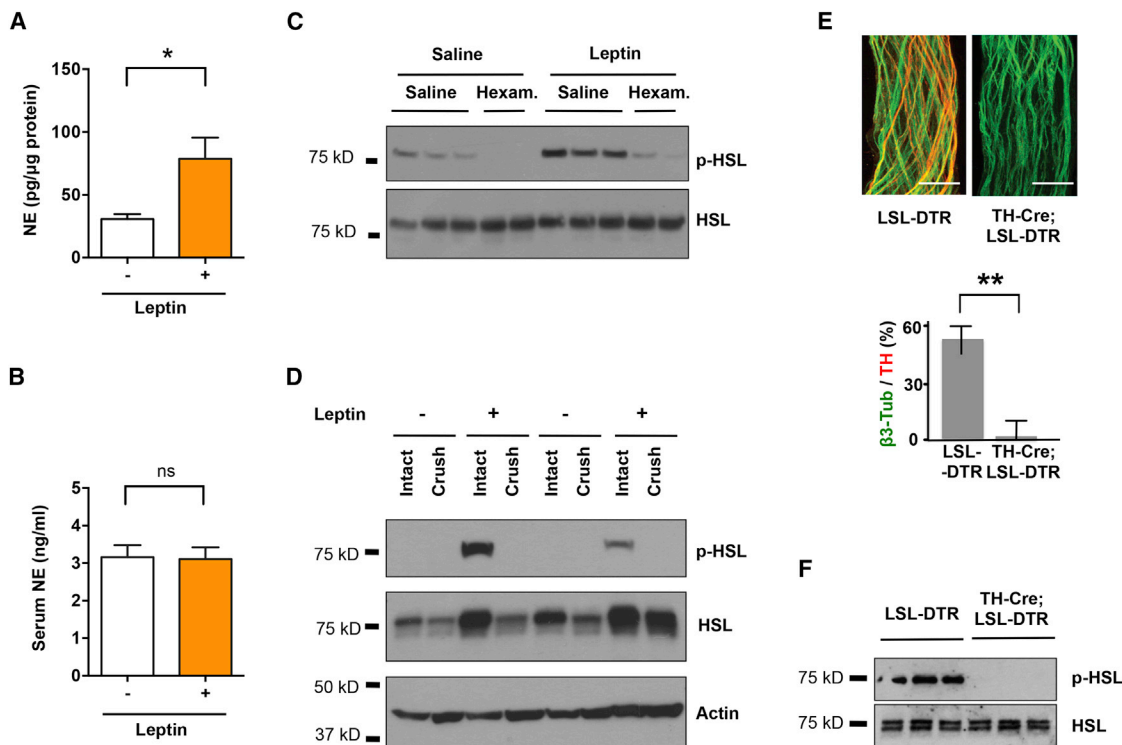


Figure 5. Sympathetic Neurons Are Locally Required for Leptin-Induced Lipolysis

(A and B) C57BL6/J mice were peripherally administrated with 500 ng/hr recombinant leptin or saline for 2 days. (A) NE content in subcutaneous fat pads ($p < 0.05$; $n = 5$) and (B) NE serum levels were measured by NE ELISA ($n = 4$). Results are shown as mean \pm SEM. ns, not significant.

(C and D) C57BL6/J mice were peripherally administrated with 500 ng/hr recombinant leptin (C) in combination with 500 μ g/hr ganglionic blocker hexamethonium (Hexam.) or (D) at 3 days after local crush injury of nerves in fat pads. p-HSL in total protein extracts of epididymal fats were examined by immunoblot analysis. (E) Fat pads in *TH-Cre; LSL-DTR* mice were locally treated with DT. Tissue-specific ablation of SNS axons confirmed by immunostaining for Tub-3 and TH (** $p < 0.001$; $n = 6$). Results are shown as mean \pm SEM.

(F) Immunoblot analysis of p-HSL in total protein extracts of subcutaneous fats of *TH-Cre; LSL-DTR* and control mice injected with DT following leptin treatment (500 ng/hr).

See also Figure S1.

low doses (10 ng/g) to ensure that the effect was local and to also spare TH-positive neurons in CNS (Figure S1; Domingos et al., 2013). Genetic ablation of sympathetic input to adipose tissue completely blocked the effect of leptin on HSL phosphorylation on the ipsilateral compared to the contralateral untreated side (Figure 5F). Together, these results demonstrate that activation of sympathetic neurons in fat is necessary for leptin to stimulate HSL phosphorylation in adipose tissue.

β -Adrenergic Signaling Influences Leptin-Stimulated Lipolysis in WAT

Consistent with a sympathetic mechanism for the leptin-mediated stimulation of lipolysis, systemic administration of the β -adrenergic agonist isoproterenol resulted in the rapid induction of p-HSL. As previously reported, isoproterenol also increased FFA release from WAT in vitro and in vivo (Figure S2). Therefore, we set out to test whether β -adrenergic signaling was required for leptin-stimulated lipolysis.

We first examined the lipolytic response to leptin in mice with a knockout (KO) of dopamine β -hydroxylase (*DBH*), a key enzyme in the synthesis of NE and epinephrine from dopamine (Figure 6).

After peripheral administration of leptin, there was a dramatic increase of HSL phosphorylation in WAT in the WT or *DBH*^{+/+} animals but a markedly diminished response in the *DBH*^{-/-} littermates (Figure 6A). Consistent with this, the total fat composition dramatically decreased in the WT mice treated with leptin, while there was only a slight change of fat mass in mice with the *DBH* deletion ($p < 0.05$; Figure 6B). Also consistent with a diminished lipolytic effect of leptin, there was also a lower amount of weight loss in the *DBH*^{-/-} mice (Figure 6C). After 2 days of leptin treatment, the body weight of WT mice decreased more than 6%, while the weight loss of *DBH*^{-/-} was less than 2% ($p < 0.05$). The data suggest that catecholamines contribute to more than 50% of leptin's effect on body weight. Altogether, the results confirm that catecholamines are required for the leptin-stimulated lipolysis and HSL phosphorylation in WAT.

To test whether the action of leptin to drive lipolysis is mediated through β -adrenergic signaling, we crossed the $\beta 1/\beta 2$ double-KO to $\beta 3$ KO to generate animals with a deletion of all three β -adrenergic receptors (Figure 7). Animals with a deletion of all three isoforms of the β -adrenergic receptors showed

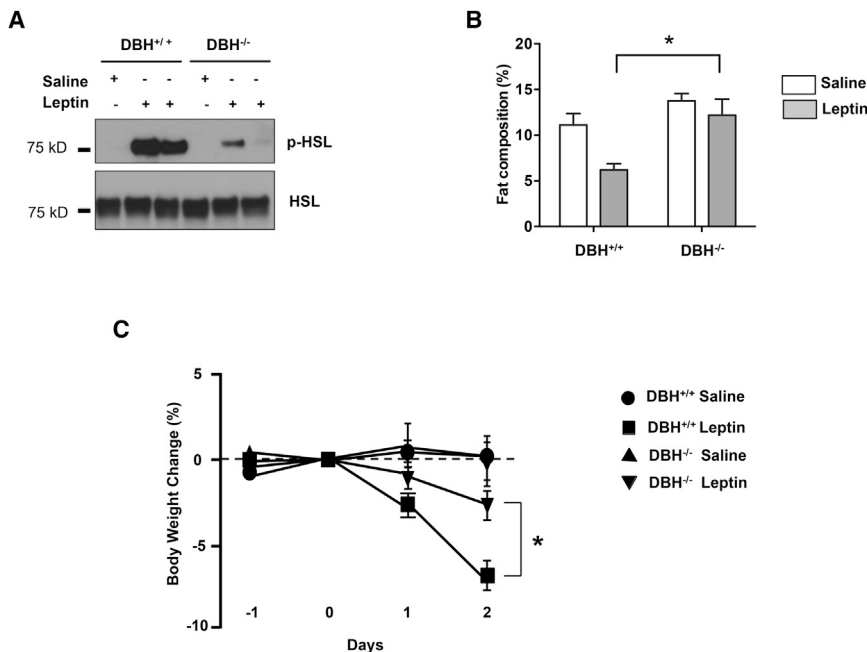


Figure 6. Norepinephrine Deficiency Impairs Leptin-Induced Lipolysis

(A) Immunoblot analysis of p-HSL in total protein extracts of fat pads of dopamine β -monooxygenase mutant and control littermates (DBH^{-/-} and DBH^{+/+}, respectively) mice that were treated with 500 ng/hr recombinant leptin.

(B) Whole-body fat composition ($*p < 0.05$). Results are shown as mean \pm SEM ($n = 4-5$).

(C) Body weight change after leptin treatment ($*p < 0.05$). Results are shown as mean \pm SEM ($n = 5$).

significantly decreased HSL phosphorylation after leptin treatment in comparison to the double-KO controls (Figure 7A). However, this decrease was not as marked as that seen in individual depots after local ablation of sympathetic fibers using DT (Figure 5F). While leptin treatment significantly decreased total fat mass in $\beta 1^{-/-}\beta 2^{-/-}$ mice, this effect was significantly reduced in $\beta 1^{-/-}\beta 2^{-/-}\beta 3^{-/-}$ triple-KO mice (Figure 7B; paired ANOVA post hoc test, $p < 0.01$, comparing $\beta 1^{-/-}\beta 2^{-/-}\beta 3^{-/-}$ with $\beta 1^{-/-}\beta 2^{-/-}\beta 3^{+/+}$ mice after leptin treatment). In contrast, α -adrenergic receptors appeared to play only a minor role in the leptin-stimulated loss of fat mass, because the α -adrenergic blockers phentolamine (5 mg/kg, intraperitoneally [i.p.]) and phenoxybenzamine (10 mg/kg i.p.) failed to diminish the catabolic responses to leptin treatment in $\beta 1^{-/-}\beta 2^{-/-}\beta 3^{+/+}$ control mice or $\beta 1^{-/-}\beta 2^{-/-}\beta 3^{-/-}$ mice (Figure 7C). There was also a small suppression of body weight loss in response to leptin in the $\beta 1^{-/-}\beta 2^{-/-}\beta 3^{-/-}$ mice (Figure 7D). These results showed that the β -adrenergic receptors are only partially necessary for leptin-mediated lipolysis of WAT but that the magnitude of the effect of a loss of β -adrenergic signaling is not as great as that observed by interfering with local neural outputs, thus suggesting that there could also be other neural mediators or interacting receptors on adipocytes (Figure 5).

DISCUSSION

Leptin is known to stimulate lipolysis and reduce fat mass, though the physiologic mechanisms responsible for this have not been fully delineated. In this study, we present data using functional, anatomic, biochemical, and genetic approaches to show that leptin increases lipolysis via the actions of sympathetic neuronal efferents to adipose tissue. These data also provide molecular, cellular, and anatomic evidence confirming the exis-

tence of neuronal projections onto adipocytes, which have been the subject of conjecture but which have not been directly visualized.

The existence of neuro-adipose junctions in WAT had been inferred based on the fact that a pseudorabies retrograde-tracing virus can visualize a set of neural projections in the brain (Bartness and Song, 2007). In addition, immunohistochemistry, and immunofluorescence have been used to visualize contacts be-

tween sympathetic neurons and adipocytes in sliced tissue (Giordano et al., 1996, 2005; Thompson, 1986). However, these methods, which require tissue slicing and fixation, do not distinguish en passant neurons from those that directly project onto adipocytes. The visualization of adipocyte-projecting neurons that can completely envelop an adipocyte has not been accomplished so far. We were able to directly visualize neural termini onto adipocytes using intra-vital multiphoton microscopy, which allows deep penetrance onto the live intact tissue, allowing us to visualize deeper structures without the perturbations associated with classical histological methods, which, in past studies, may have compromised the integrity of the neuro-adipose termini (Helmchen and Denk, 2005).

Confocal or multiphoton microscopy methods are suitable for histological analysis at a microscopic spatial scale, but do not give a 3D perspective of the organization of the organ as a whole. At a macroscopic spatial scale, methods such as MRI or computed tomography (CT) allow for measurement of whole-body fat distribution. However, all of these methods lack the spatial resolution that is required for visualizing structures such as nerve bundles. OPT is a technique with physical principles similar to those of X-ray CT/gamma radiation, which uses visible light instead of radiation (Gualda et al., 2013). Scattering of light passing through tissues is minimized by clearing lipids from the whole organ (Quintana and Sharpe, 2011). Unlike most currently available methods, OPT coupled to tissue clearing allows imaging of whole-mount samples with a spatial scale in the order of centimeters.

It has been previously shown that electrical stimulation of WAT nerve bundles can drive lipolysis (Correll, 1963). However, as shown here, nerve bundles in WAT have mixed molecular identity, making it difficult to ascertain the identity of the neurons responsible for this effect. To address this limitation, we used

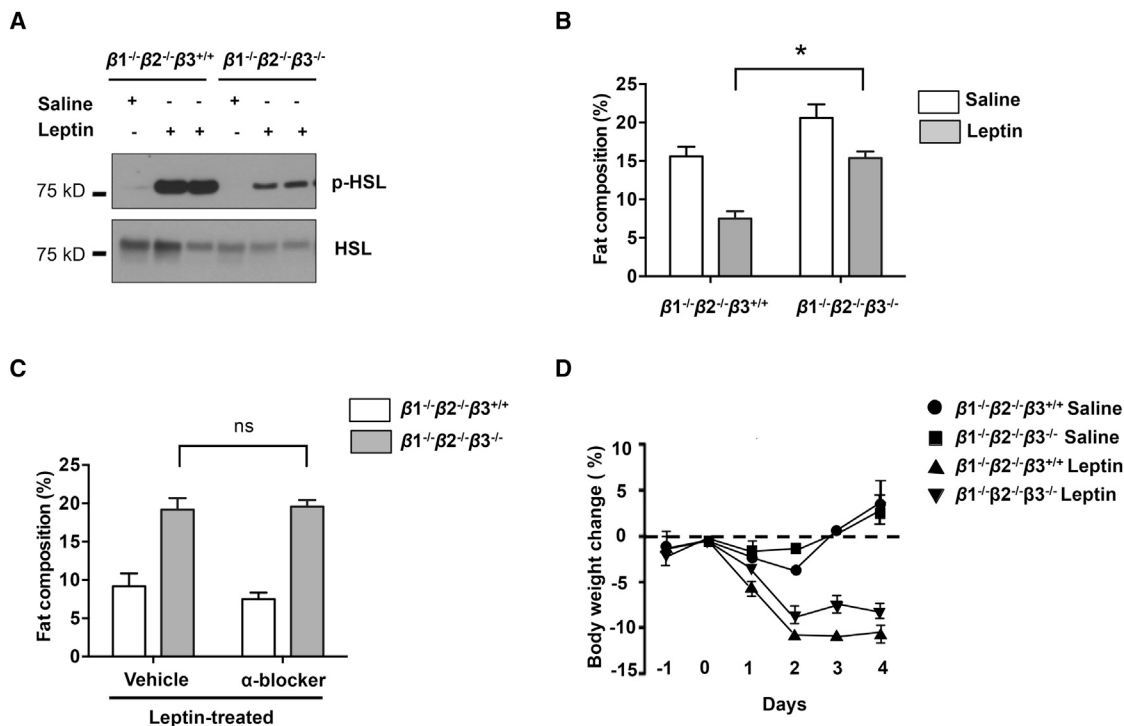


Figure 7. Deficiency of All β -Adrenergic Receptors Influences Leptin-Induced Lipolysis

(A) Immunoblot analysis of p-HSL in total protein extracts of fat pads of $\beta 1^{-/-}\beta 2^{-/-}\beta 3^{+/+}$ and $\beta 1^{-/-}\beta 2^{-/-}\beta 3^{-/-}$ mice that were treated with 500 ng/hr recombinant leptin.

(B) Whole-body fat composition (* $p < 0.05$, $n = 4-5$). Results are shown as mean \pm SEM.

(C) α -Adrenergic receptors had a minor function in leptin-induced lipolysis (* $p > 0.05$, $n = 4-5$). Results are shown as mean \pm SEM. ns, not significant.

(D) Whole-body fat composition of mice peripherally treated with recombinant leptin and α -blockers (phenolamine, 5 mg/kg, i.p.; and phenoxybenzamine, 10 mg/kg, i.p.) was measured ($n = 4-5$). Results are shown as mean \pm SEM.

See also Figure S2.

optogenetics, which allows for cell-specific stimulation of neurons (Domingos et al., 2011, 2013). In the present study, we used optogenetics to specifically activate sympathetic neurons in *TH-Cre* mice. Another advantage of this approach is that it enables the specific activation of axonal projections and does not require stimulation of neuronal cell bodies (Petreanu et al., 2007; Vrontou et al., 2013). This feature is particularly convenient for autonomic neurons, given the deep localization of their cell bodies along the anterior face of the spinal cord and the intrinsic difficulty of implanting optical fibers in this location. Previous studies using neural tracing have revealed that sympathetic neurons innervating the subcutaneous inguinal fat pads localize to the 13th thoracic ganglia, which localizes at the dorsal edge of the diaphragm muscle, in the transition between the thorax and the abdomen (Youngstrom and Bartness, 1995). This anatomical location is particularly inaccessible and unsuitable for chronic implants of optical fibers or equivalent devices. However, as we show here, subcutaneous implant of optical fibers for stimulation of nerve terminals is feasible and effective. We used this approach to show that optogenetic gain of function of the catecholaminergic signaling to the neuro-adipose junction can lead to the phosphorylation of HSL and lipolysis of WAT. Similarly, previous loss-of-function experiments that assessed the effect of

sympathetic input on lipolysis also did not allow analysis of the effect of specific cells in the way that optogenetics can. Thus, the use of mechanical denervation does not distinguish between neurons that directly innervate adipocytes versus those that are passing through. We have not yet profiled the non-TH nerve fibers, but it is reasonable to expect that some might be parasympathetic, nociceptive, sensory fibers and/or en passant axons. The function of these fibers could be assessed similarly to those that we report, using optogenetics, to activate other populations, including cholinergic neurons, by studying choline acetyltransferase (ChAT)-Cre mice and/or neurons expressing other molecular markers. Chemical ablation with capsaicin also has limitations, as this treatment is not specific to sympathetic neurons and affects all transient-receptor-potential-vanilloid (TRPV)-expressing fibers (Holzer, 1991). Chemical ablation with 6-hydroxydopamine is likely to affect dopaminergic as well as enteric neurons, creating secondary systemic effects (Ding et al., 2004).

To avoid these limitations and gain local control over sympathetic neural activity, we used additional molecular genetic tools that combine tissue specificity with a localized effect. We show that ablation of the sympathetic neurons by DTR expression in TH-positive neurons followed by local DT injection in WAT abolishes the effect of leptin on HSL phosphorylation. We also noted

that the loss of function due to post-synaptic manipulations (i.e., the triple β -adrenergic receptor KO in Figure 7) has a lesser effect on the size of adipose tissue depots than that seen after pre-synaptic manipulations such as a loss of *DBH* or pharmacologic or mechanical ablation of neural input to fat (Figure 6). This suggests that leptin-induced production of NE from sympathetic neurons could act through additional receptors that are not one of the three β -adrenergic receptors that we tested, which have been suggested by others (Tavernier et al., 2005). Alternatively, sympathetic neurons may co-release other neurotransmitters or neuropeptides that signal through non-adrenergic receptors. This could account for the residual leptin-induced weight loss seen in *DBH*^{-/-}, although this effect is not significant when compared to controls. Thus, an in-depth knowledge of the underlying sympathetic neural circuits could provide strategies to pharmacologically activate specific sympathetic neuronal population, thus circumventing leptin resistance, as potential treatment of obesity.

A canonical effect of leptin is to increase sympathetic signaling to BAT, thus promoting thermogenesis (Bachman et al., 2002; Landsberg et al., 1984). However the role of autonomic stimulation of white fat has been less well studied. We now show that the sympathetic activity is also responsible for the leptin-stimulated lipolysis in WAT. While leptin has been assumed to increase lipolysis via activation of sympathetic efferent fibers, this has not been directly shown. Adrenergic agonists have been shown to induce the formation of beige (brite) fat, and these data suggest that sympathetic innervation may also stimulate this phenotypic change in adipose tissue (Bachman et al., 2002; Giralto and Villarroya, 2013; Dempersmier et al., 2015). Consistent with this, leptin has also been suggested to increase the formation of beige fat (Dodd et al., 2015).

Because brown adipocytes have relatively smaller fat storages compared to white adipocytes, while having higher metabolic demand, the continuous thermogenic response of BAT might require the supply of FFA from WAT mobilized in other parts of the body. Therefore, it is reasonable to speculate that the coordinated sympathetic actions in BAT and WAT in response to leptin could help maximize the hormone's effect on energy expenditure and fat metabolism. Future studies delineating the neural circuits connecting the central action of leptin with the peripheral activation of sympathetic system will be necessary to test this hypothesis. Particularly, it would be of great importance to develop technologies that would allow whole-body visualization and mapping of peripheral neuronal circuits using some of the approaches presented here.

In summary, we provide direct evidence that the sympathetic neuro-adipose junction is both necessary and sufficient for leptin to drive lipolysis in WAT.

EXPERIMENTAL PROCEDURES

Antibodies and Drugs

The antibodies were obtained from the following vendors: HSL (Cell Signaling Technology), phospho-HSL (Cell Signaling Technology), phospho-PKA substrate (Cell Signaling Technology), TH (Pel-Freez Biologicals), and actin (Sigma). Hexamethonium chloride, phentolamine, and phenoxybenzamine were from Sigma-Aldrich. DT was purchased from Merck Millipore. Recombinant mouse leptin was obtained from Amylin Pharmaceuticals.

Mice

DBH KO mice were kindly provided by Steve Thomas at the University of Pennsylvania. *Adrb1*^{-/-} *2*^{-/-} and *Adrb3*^{-/-} were kindly provided by Bruce Spiegelman at Harvard Medical School. *TH-Cre*, Rosa26-LSL-ChR2-YFP (Stock No. 012-569; Daou et al., 2013), Rosa26-LSL-DTR, and C57BL/6J mice at 6–10 weeks old were purchased from The Jackson Laboratory. Animal procedures were approved by the ethics committee of Instituto Gulbenkian de Ciéncia and the Institutional Animal Care and Use Committee of Rockefeller University.

OPT

Six-week-old C57BL/6 mice were sacrificed with carbon dioxide. The inguinal fat pads were dissected from the mice with Dumont #5 Forceps, fixed in 4% paraformaldehyde (PFA; Sigma-Aldrich) for 3 hr at room temperature (RT) and subjected to the OPT clearing protocol as described in the Supplemental Experimental Procedures. Images of the whole fat tissue were acquired using a 1× lens mounted on an Infinitube tube lens and projected into a Hamamatsu FlashLT sCMOS camera. A total of 1,600 images were acquired for a full rotation (0.25° steps). The series of projections were then pre-processed for back-projection using FIJI in order to remove hot pixels and re-align the axis of rotation in relation to the camera chip, and finally the back-projection reconstruction was conducted using the Skyscan's NRecon software (Schindelin et al., 2012). The stack of slices was further processed with FIJI to increase contrast and saved to posterior analysis with the software Amira V5.3. Using this software, 3D reconstructions and image segmentation were performed to identify and reconstruct individual parts of the fat organs. Detailed instructions for setting up an OPT system can be found at <https://sites.google.com/site/openspinmicroscopy/home/opt>.

In Vivo Two-Photon Microscopy

Two-month-old mice were kept anesthetized with 2% isoflurane. During surgery, body temperature was maintained at 37°C with a warming pad. After application of local anesthetics (lidocaine), a sagittal incision of the skin was made above the supra-pelvic flank to expose the subcutaneous inguinal fat pad. An imaging chamber was custom built to minimize fat movement. Warm imaging solution (in millimolar: 130 NaCl, 3 KCl, 2.5 CaCl₂, 0.6 MgCl₂ · 6H₂O, 10 HEPES without Na, 1.2 NaHCO₃, 10 glucose (pH 7.45), with NaOH) (37°C) mixed with a fat dye (LipidTOX) was applied to label adipocytes, maintain tissue integrity, and allow the use of immersion objective. Imaging experiments were performed under a two-photon laser-scanning microscope (Ultima, Prairie Instruments). Live images were acquired at 8–12 frames per second, at depths below the surface ranging from 100 to 250 μ m, using an Olympus 20× 0.8 N.A. water immersion objective, with a laser tuned to 860–940 nm wavelength, and emission filters 525/50 nm and 595/50 nm for green and red fluorescence, respectively. Laser power was adjusted to be 20–25 mW at the focal plane (maximally, 35 mW), depending on the imaging depth and level of expression of dtTomato and LipidTOX spread. tdTomato fluorescence was used to identify TH-positive fibers until photobleaching occurred.

Leptin Treatment and Lipolysis Analysis

To examine the effect of leptin treatment on lipolysis, leptin (delivery rate of 500 ng/hr) or saline was delivered through osmotic pumps (Alzet) subcutaneously for 2 days. Body weight was recorded daily. Body fat composition was measured using the EchoMRI body analyzer at end point before subcutaneous or epididymal adipose tissues were collected. HSL phosphorylation was detected by immunohistochemistry of paraffin sections at 6- μ m thickness and/or western blot of subcutaneous or epididymal adipose tissues. NE levels in serum and subcutaneous fat pads were determined with an NE ELISA kit (Labor Diagnostika Nord GmbH). Tissues were homogenized and sonicated in homogenization buffer (1 N HCl, 1 mM EDTA), and cellular debris was pelleted by centrifugation at 13,000 rpm for 15 min at 4°C. All tissue samples were normalized to total tissue protein concentration.

Mechanical Denervation

The nerve bundle 2 mm distal from the tip of the epididymal fat was physically crushed for 30 s and then released using a forcep. Leptin was administered through osmotic pump 3 days after nerve crush. HSL phosphorylation was detected 2 days upon leptin treatment.

Hexamethonium Chloride, Isopreterenol, and α -Blocker Treatment

Hexamethonium chloride (500 μ g/hr) was administered during leptin treatment through a separate osmotic pump, and the α -blockers phentolamine (5 mg/kg, intraperitoneally [i.p.]) and phenoxybenzamine (10 mg/kg; i.p.) were administered twice a day during the course of leptin treatment (500 ng/hr). Isopreterenol (250 μ g per mouse) was delivered in saline through jugular vein injection. Blood was drawn through tail bleeding, and plasma FFA was measured using a NETO kit (Wako Pure Chemicals Industries). For FFA release upon isopreterenol treatment in vitro, adipose tissue explants were dissected and cultured in Hank's medium and stimulated with isopreterenol at 10 μ g/ml for 3 hr. FFA was measured in the medium.

NE Measurements after Optogenetic Stimulation Ex Vivo

SCG were removed from 28- to 30-day-old *TH-Cre X Rosa26-LSL-ChR2-YFP* mice under a stereomicroscope and placed in DMEM (Invitrogen). Ganglia were cleaned from the surrounding tissue capsule and transferred into eight-well tissue culture chambers (Sarstedt) that were previously coated with poly-D-lysine (Sigma-Aldrich) in accordance to the manufacturer's instructions. Ganglia were then covered with 5 μ l Matrigel (BD Biosciences) and incubated for 7 min at 37°C. DMEM without phenol red (Invitrogen) supplemented with 10% fetal bovine serum (Invitrogen), 2 mM L-glutamine (Biowest), and nerve growth factor (Sigma-Aldrich) was subsequently added. SCG ganglia were cultured for a minimum of 24 hr prior to further manipulation. Depolarization of sympathetic neurons in explant cultures was performed on a Yokogawa CSU-X1 Spinning Disk confocal system using the 488-nm laser line and pointing at the region of interest (ROI) for 200 μ s. Stimulation was repeated five times using 40% of laser intensity. NE in the SCG explant culture medium was determined with an NE ELISA kit (Labor Diagnostika Nord GmbH). The same procedure was performed for *LSL-ChR2-YFP* control mice.

Surgeries and Optogenetic Stimulation

General anesthesia was induced and maintained with isoflurane. After application of local anesthetics (lidocaine), a sagittal incision of the skin was made above the neck and supra-pelvic flank. A hemostat was inserted into the incision and, by opening and closing the jaws of the hemostat, spread the subcutaneous tissue to create a longitudinal pocket for the optical fiber. The pocket was made long enough to allow about 4–6 cm of fiber (Thorlabs FT200). The tip of the fiber targeted the anatomical location of the inguinal fat pad. The other end of the fiber, the ferrule-connector end, was secured along the skin via sutures and dermal staples. Appropriate local analgesic was used post-surgically. Optogenetic stimulations were performed 48 hr after surgical procedures.

The stimulation session in Figure 4D lasted 4–6 hr and was performed via a 1-s 20-Hz pulse of blue laser every other second, originating from a 473-nm solid laser source (OEM-BL-473-00100-CWM-SD-05). The laser source had an output power of 100 mW. Ferrule-coupled optical fibers of 200- μ m diameter (Thorlabs; FT200EMT-CANNULA-TS1031629) were connected to ferrule patch cords (Thorlabs; FT200EMT-FC/PC-ferrule) with mating sleeves (Thorlabs; ADAF1), and the later to the laser source via FC/PC adaptor.

NE in subcutaneous fat pads was determined with an NE ELISA kit (Labor Diagnostika Nord GmbH) as described earlier.

Stimulation protocol in Figure 4E took place every day for 2 weeks and solely during the rodent rest period. Longer sessions, as in Figure 4F, had a duration of 4 weeks. Stimulation sessions lasted 4–6 hr and were performed as described earlier.

MRI Fat Measurements and Fat Pad Segmentation

Mice were subjected to optogenetic stimulation as stated earlier, perfused with 4% PFA/PBS, post-fixed over 2–3 days, and embedded in Fomblin Oil (Sigma-Aldrich) for scanning. Imaging was performed on a 7.0 T 70/30 Bruker Biospec small-animal MRI system with a 12-cm diameter 450 mT/m amplitude and 4,500 T/m/s slew rate actively shielded gradient subsystems with integrated shim capability. A linear coil with 7-cm diameter and a length sufficient to cover the whole body of the animal was used for excitation and reception of the magnetic resonance signal. Two image sets were acquired, one with fat suppression and one without. Axial images, covering the whole animal in 75 0.4-mm-thick slices without gap, were acquired in an interleaved

way by using a RARE (rapid acquisition with relaxation enhancement) pulse sequence with RARE factor 2. Four averages with a flip angle of 90°—echo time (TE) = 10 ms, repetition time (TR) = 2,468 ms, field of view = 10 \times 3 cm, and matrix size = 256 \times 128 (acquisition matrix size = 256 \times 96), resulting in a spatial resolution of 0.391 \times 0.234 \times 0.4 mm—were acquired. The fat suppression, added to the second scan, consists of a 90° Gaussian pulse with 2.6067-ms duration and 1051.1-Hz bandwidth. Data were converted into .tif files by FIJI software. The subcutaneous inguinal fat distribution was determined with semi-automated Amira V5.3 software segmentation of scanned images. Amira V5.3 software segmentation relies on the automated grouping of pixels with the same index of intensity in the grayscale. An automatic segmentation based on the gray threshold levels, which decomposes the image domain into subsets, allowed us to define the right and the left inguinal fat depots, which were further saved as unique fields. Volumes of the right and the left subcutaneous fat pads were defined as the number of voxels multiplied by the size of a single voxel. The size of stimulated fat pads was determined, and the effect of optogenetic stimulation of neurons on fat mass was calculated in the same animal relative to non-stimulated contralateral side.

Statistical Methods

Statistics were performed in GraphPad Prism and involved the computation of means and SEM, which accompany each figure legend. Student's *t* tests and ANOVAs were used where appropriate, and *p* values are indicated in text.

SUPPLEMENTAL INFORMATION

Supplemental Information includes Supplemental Experimental Procedures, two figures, and two movies and can be found with this article online at <http://dx.doi.org/10.1016/j.cell.2015.08.055>.

AUTHOR CONTRIBUTIONS

Two-photon microscopy and optogenetics were performed by A.I.D. and R.M.P., and related rodent husbandry was performed by N.K. and E.S. OPT was performed by R.M.P., M.M.A.P., and G.G.M.; MRI scans were conducted by H.V.; Amira segmentation of MRI data was performed by R.M.P. and M.M.A.P.; cell cultures and neuronal explants were developed by A.B. and R.M.P. Biochemical analyses and measurement of whole body fat composition and body weights were performed by W.Z., N.K., E.S., Y.H.L., and A.K.; A.I.D. and J.M.F. wrote the manuscript.

ACKNOWLEDGMENTS

This work was supported by the Fundação para a Ciência e Tecnologia (FCT), the European Molecular Biology Organization (EMBO), and the JPB Foundation. The FCT supported A.I.D., R.M.P., M.M.A.P., N.K., G.G.M., A.B., and E.S. The JPB Foundation supported the work of W.Z., Y.H.L., and A.K. J.M.F. is a Howard Hughes Medical Institute (HHMI) investigator.

Received: May 6, 2015

Revised: July 17, 2015

Accepted: August 6, 2015

Published: September 24, 2015

REFERENCES

- Arvaniti, K., Deshaies, Y., and Richard, D. (1998). Effect of leptin on energy balance does not require the presence of intact adrenals. *Am. J. Physiol.* 275, R105–R111.
- Awad, S., Constantin-Teodosiu, D., Macdonald, I.A., and Lobo, D.N. (2009). Short-term starvation and mitochondrial dysfunction - a possible mechanism leading to postoperative insulin resistance. *Clin. Nutr.* 28, 497–509.
- Bachman, E.S., Dhillon, H., Zhang, C.Y., Cinti, S., Bianco, A.C., Kobilka, B.K., and Lowell, B.B. (2002). betaAR signaling required for diet-induced thermogenesis and obesity resistance. *Science* 297, 843–845.

- Bartness, T.J., and Song, C.K. (2007). Thematic review series: adipocyte biology. Sympathetic and sensory innervation of white adipose tissue. *J. Lipid Res.* *48*, 1655–1672.
- Bartness, T.J., Kay Song, C., Shi, H., Bowers, R.R., and Foster, M.T. (2005). Brain-adipose tissue cross talk. *Proc. Nutr. Soc.* *64*, 53–64.
- Brasaemle, D.L. (2007). Thematic review series: adipocyte biology. The perilipin family of structural lipid droplet proteins: stabilization of lipid droplets and control of lipolysis. *J. Lipid Res.* *48*, 2547–2559.
- Buch, T., Heppner, F.L., Tertilt, C., Heinen, T.J., Kremer, M., Wunderlich, F.T., Jung, S., and Waisman, A. (2005). A Cre-inducible diphtheria toxin receptor mediates cell lineage ablation after toxin administration. *Nat. Methods* *2*, 419–426.
- Correll, J.W. (1963). Adipose tissue: ability to respond to nerve stimulation in vitro. *Science* *140*, 387–388.
- Daou, I., Tuttle, A.H., Longo, G., Wieskopf, J.S., Bonin, R.P., Ase, A.R., Wood, J.N., De Koninck, Y., Ribeiro-da-Silva, A., Mogil, J.S., and Séguéla, P. (2013). Remote optogenetic activation and sensitization of pain pathways in freely moving mice. *J. Neurosci.* *33*, 18631–18640.
- Dempersmier, J., Sambeat, A., Gulyaeva, O., Paul, S.M., Hudak, C.S., Raposo, H.F., Kwan, H.Y., Kang, C., Wong, R.H., and Sul, H.S. (2015). Cold-inducible Zfp516 activates UCP1 transcription to promote browning of white fat and development of brown fat. *Mol. Cell* *57*, 235–246.
- Ding, Y.M., Jaumotte, J.D., Signore, A.P., and Zigmond, M.J. (2004). Effects of 6-hydroxydopamine on primary cultures of substantia nigra: specific damage to dopamine neurons and the impact of glial cell line-derived neurotrophic factor. *J. Neurochem.* *89*, 776–787.
- Dodd, G.T., Decherf, S., Loh, K., Simonds, S.E., Wiede, F., Bolland, E., Merry, T.L., Münzberg, H., Zhang, Z.Y., Kahn, B.B., et al. (2015). Leptin and insulin act on POMC neurons to promote the browning of white fat. *Cell* *160*, 88–104.
- Domingos, A.I., Vaynshteyn, J., Voss, H.U., Ren, X., Gradinaru, V., Zang, F., Deisseroth, K., de Araujo, I.E., and Friedman, J. (2011). Leptin regulates the reward value of nutrient. *Nat. Neurosci.* *14*, 1562–1568.
- Domingos, A.I., Sordillo, A., Dietrich, M.O., Liu, Z.W., Tellez, L.A., Vaynshteyn, J., Ferreira, J.G., Ekstrand, M.I., Horvath, T.L., de Araujo, I.E., and Friedman, J.M. (2013). Hypothalamic melanin concentrating hormone neurons communicate the nutrient value of sugar. *eLife* *2*, e01462.
- Elia, M., Stubbs, R.J., and Henry, C.J. (1999). Differences in fat, carbohydrate, and protein metabolism between lean and obese subjects undergoing total starvation. *Obes. Res.* *7*, 597–604.
- Friedman, J.M., and Halaas, J.L. (1998). Leptin and the regulation of body weight in mammals. *Nature* *395*, 763–770.
- Giordano, A., Morroni, M., Santone, G., Marchesi, G.F., and Cinti, S. (1996). Tyrosine hydroxylase, neuropeptide Y, substance P, calcitonin gene-related peptide and vasoactive intestinal peptide in nerves of rat periovarian adipose tissue: an immunohistochemical and ultrastructural investigation. *J. Neurocytol.* *25*, 125–136.
- Giordano, A., Frontini, A., Murano, I., Tonello, C., Marino, M.A., Carruba, M.O., Nisoli, E., and Cinti, S. (2005). Regional-dependent increase of sympathetic innervation in rat white adipose tissue during prolonged fasting. *J. Histochem. Cytochem.* *53*, 679–687.
- Giralt, M., and Villarroya, F. (2013). White, brown, beige/brite: different adipose cells for different functions? *Endocrinology* *154*, 2992–3000.
- Gualda, E.J., Vale, T., Almada, P., Feijó, J.A., Martins, G.G., and Moreno, N. (2013). OpenSpinMicroscopy: an open-source integrated microscopy platform. *Nat. Methods* *10*, 599–600.
- Halaas, J.L., Gajiwala, K.S., Maffei, M., Cohen, S.L., Chait, B.T., Rabinowitz, D., Lallone, R.L., Burley, S.K., and Friedman, J.M. (1995). Weight-reducing effects of the plasma protein encoded by the obese gene. *Science* *269*, 543–546.
- Halaas, J.L., Boozer, C., Blair-West, J., Fidathusein, N., Denton, D.A., and Friedman, J.M. (1997). Physiological response to long-term peripheral and central leptin infusion in lean and obese mice. *Proc. Natl. Acad. Sci. USA* *94*, 8878–8883.
- Helmchen, F., and Denk, W. (2005). Deep tissue two-photon microscopy. *Nat. Methods* *2*, 932–940.
- Holzer, P. (1991). Capsaicin: cellular targets, mechanisms of action, and selectivity for thin sensory neurons. *Pharmacol. Rev.* *43*, 143–201.
- Koffler, M., and Kisch, E.S. (1996). Starvation diet and very-low-calorie diets may induce insulin resistance and overt diabetes mellitus. *J. Diabetes Complications* *10*, 109–112.
- Landsberg, L., Saville, M.E., and Young, J.B. (1984). Sympathoadrenal system and regulation of thermogenesis. *Am. J. Physiol.* *247*, E181–E189.
- Montez, J.M., Soukas, A., Asilmaz, E., Fayzikhodjaeva, G., Fantuzzi, G., and Friedman, J.M. (2005). Acute leptin deficiency, leptin resistance, and the physiologic response to leptin withdrawal. *Proc. Natl. Acad. Sci. USA* *102*, 2537–2542.
- Newman, W.P., and Brodows, R.G. (1983). Insulin action during acute starvation: evidence for selective insulin resistance in normal man. *Metabolism* *32*, 590–596.
- Nguyen, K.D., Qiu, Y., Cui, X., Goh, Y.P., Mwangi, J., David, T., Mukundan, L., Brombacher, F., Locksley, R.M., and Chawla, A. (2011). Alternatively activated macrophages produce catecholamines to sustain adaptive thermogenesis. *Nature* *480*, 104–108.
- Petreanu, L., Huber, D., Sobczyk, A., and Svoboda, K. (2007). Channelrhodopsin-2-assisted circuit mapping of long-range callosal projections. *Nat. Neurosci.* *10*, 663–668.
- Quintana, L., and Sharpe, J. (2011). Optical projection tomography of vertebrate embryo development. *Cold Spring Harb. Protoc.* *2011*, 586–594.
- Rafael, J., and Herling, A.W. (2000). Leptin effect in ob/ob mice under thermoneutral conditions depends not necessarily on central satiation. *Am. J. Physiol. Regul. Integr. Comp. Physiol.* *278*, R790–R795.
- Rezaei-Zadeh, K., and Münzberg, H. (2013). Integration of sensory information via central thermoregulatory leptin targets. *Physiol. Behav.* *121*, 49–55.
- Scarpace, P.J., and Matheny, M. (1998). Leptin induction of UCP1 gene expression is dependent on sympathetic innervation. *Am. J. Physiol.* *275*, E259–E264.
- Schindelin, J., Arganda-Carreras, I., Frise, E., Kaynig, V., Longair, M., Pietzsch, T., Preibisch, S., Rueden, C., Saalfeld, S., Schmid, B., et al. (2012). Fiji: an open-source platform for biological-image analysis. *Nat. Methods* *9*, 676–682.
- Tavernier, G., Jimenez, M., Giacobino, J.P., Hulo, N., Lafontan, M., Muzzin, P., and Langin, D. (2005). Norepinephrine induces lipolysis in beta1/beta2/beta3-adrenoceptor knockout mice. *Mol. Pharmacol.* *68*, 793–799.
- Thompson, G.E. (1986). Vascular and lipolytic responses of the inguinal fat pad of the sheep to adrenergic stimulation, and the effects of denervation and autotransplantation. *Q. J. Exp. Physiol.* *71*, 559–567.
- Vrontou, S., Wong, A.M., Rau, K.K., Koerber, H.R., and Anderson, D.J. (2013). Genetic identification of C fibres that detect massage-like stroking of hairy skin in vivo. *Nature* *493*, 669–673.
- Weisberg, S.P., McCann, D., Desai, M., Rosenbaum, M., Leibel, R.L., and Ferrante, A.W., Jr. (2003). Obesity is associated with macrophage accumulation in adipose tissue. *J. Clin. Invest.* *112*, 1796–1808.
- Youngstrom, T.G., and Bartness, T.J. (1995). Catecholaminergic innervation of white adipose tissue in Siberian hamsters. *Am. J. Physiol.* *268*, R744–R751.

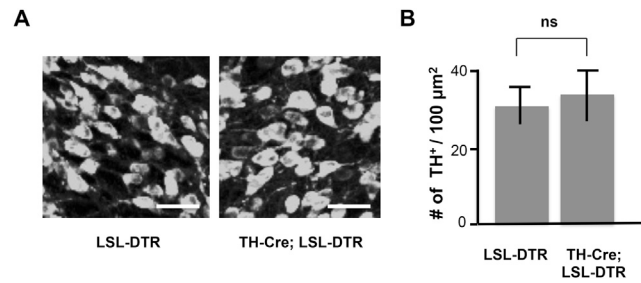


Figure S1. Local Injection of DT in Inguinal Fat Preserves TH-Positive Neurons in the Brain, Related to Figure 5

(A) Staining of TH positive neurons in brains of *Rosa26-LSL-DTR* (left) and *TH-Cre; Rosa26-LSL-DTR* mice which were locally injected in inguinal fat pads with DT.
(B) Quantification of TH-positive cell bodies per area of photomicrograph. Results are shown as mean ± SEM.

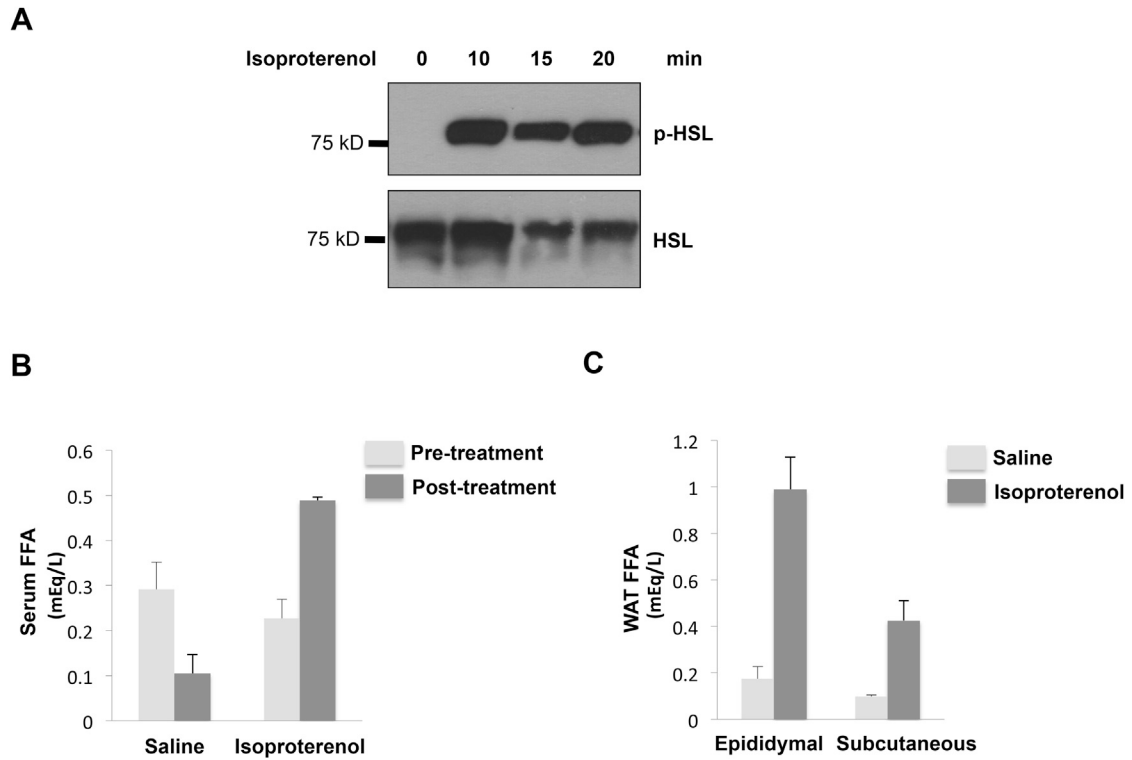


Figure S2. Activation of β -Adrenergic Signal Led to Lipolysis in WAT, Related to Figure 7

(A) Peripheral administration of β -agonist (isoproterenol) induced HSL phosphorylation.

(B) Peripheral administration of β -agonist (isoproterenol) induced release of FFA in WAT.

(C) β -agonist led to release of FFA in WAT in vitro.

Cell

Supplemental Information

Sympathetic Neuro-adipose Connections

Mediate Leptin-Driven Lipolysis

Wenwen Zeng, Roksana M. Pirzgalska, Mafalda M.A. Pereira, Nadiya Kubasova, Andreia Barateiro, Elsa Seixas, Yi-Hsueh Lu, Albina Kozlova, Henning Voss, Gabriel G. Martins, Jeffrey M. Friedman, and Ana I. Domingos

SUPPLEMENTAL EXPERIMENTAL PROCEDURES

OPT clearing

The adipose organ was fixed in 4 % paraformaldehyde (Sigma-Aldrich) for 3 h at room temperature (RT) with agitation, followed by 15 min wash step with Phosphate Buffered Saline (PBS) 1X at RT. The wash step was repeated two more times. The sample was placed in 1 % low melting agarose (Sigma-Aldrich). The agarose volume was approximately 24.5 cm³ (3.5 cm height and 1.5 cm diameter). The inguinal fat pad was immersed in a 10 % methanol (VWR) solution for 2 h at RT (with agitation). Afterwards 10 % increasing steps were performed every day until dehydration in 100 % methanol was reached (RT with agitation). The replacement of the methanol with 1:2 mixture of benzyl alcohol (Merck) and benzyl benzoate (Merck) was performed in 15 % increasing steps every day until clarification was reached.

Sympathetic neuronal cultures

Sympathetic neurons of primary cultures of SCG were performed from postnatal day 30 *TH-Cre X Rosa26-LSL-ChR2-YFP* mice. Briefly, after decapitation, both SCG of each animal were removed and cleaned of all visible adipose tissue and surrounding connective tissue before transfer to Hank's Balanced Salt Solution (HBSS). Then, SCG were treated enzymatically in two steps to yield single neurons. First, SCG were subjected to enzymatic dissociation in collagenase solution (2.5 mg/mL) in HBSS, followed by trypsin solution (0.25 %) in PBS at 37 °C with agitation. The SCG were next mechanically dissociated into a suspension of single cells. Isolated sympathetic cells were plated in a final concentration of 2500 cells per coverslip (6 mm) coated with poly-D-lysine and growth factor-reduced Matrigel, and cultured for 7 days *in vitro* (DIV) in Neurobasal medium supplemented with 2 % B-27, 10 % fetal bovine serum, 1 % penicillin/streptomycin, nerve growth factor

(100 ng/mL) and 5-fluoro-2'-deoxyuridine (5 μ M).

DT injections

General anesthesia was induced and maintained with isoflurane. After application of local anesthetics (lidocaine), a small incision of the skin was made above the supra-pelvic flank. A Hamilton syringe (10 μ l) is inserted into the incision aiming at the inguinal WAT. Each DT injection is made slowly, over period of 30 minutes. Posology was 10 ng/g.